ELSEVIER

Available online at www.sciencedirect.com

SCIENCE DIRECT®

Catalysis Today 85 (2003) 235–249

CATALYSIS TODAY

www.elsevier.com/locate/cattod

Ruthenium as oxidation catalyst: bridging the pressure and material gaps between ideal and real systems in heterogeneous catalysis by applying DRIFT spectroscopy and the TAP reactor

J. Aßmann, E. Löffler, A. Birkner, M. Muhler*

Ruhr-Universität Bochum, Lehrstuhl für Technische Chemie, D-44780 Bochum, Germany

Abstract

Two supported Ru catalysts were prepared by the chemical vapor deposition of $Ru_3(CO)_{12}$ on MgO and SiO_2 (MOCVD). TEM, XRD, and static H_2 chemisorption measurements confirmed that the Ru particle size was about 2 nm on both supports. Using in situ DRIFT (diffuse reflectance infrared Fourier transform) spectroscopy at atmospheric pressure it was found that the adsorption of CO on the reduced samples is clearly influenced by the supports whereas the adsorption of CO on the oxidized Ru catalysts is essentially independent of the support. O_2 chemisorption measurements showed that a thin RuO_2 surface layer was formed on both catalysts under oxidizing conditions at room temperature. The observed C–O stretching frequencies were found to be in good agreement with HREELS and LEED data reported for the $RuO_2(1\,1\,0)$ single crystal surface. The catalytic activity was assessed under high-vacuum conditions using the TAP (temporal analysis of products) reactor by co-feeding CO and O_2. These conditions ensured that heat and mass transfer limitations were absent. Both supported Ru catalysts were found to be highly active and stable under the CO oxidation conditions even down to room temperature. The deactivation of the catalysts observed at room temperature was reversible and independent of the support. The turnover frequencies (number of CO_2 molecules per metal surface site per second) derived from steady-state measurements are in good agreement with data reported for the $RuO_2(1\,1\,0)$ single crystal surface under UHV conditions. Based on the results of the DRIFTS (diffuse reflectance infrared Fourier transform spectroscopy) and the kinetic measurements supported RuO_2 is identified as the catalytically active phase. In addition, the turnover frequencies are in good agreement with data reported for Ru/SiO_2 at atmospheric pressure. Thus, both the materials and the pressure gap were bridged successfully.

Keywords: CO oxidation; CO adsorption; Supported Ru catalysts; DRIFT spectroscopy; TAP reactor; Metallic oxide

1. Introduction

It is still an exciting challenge to close the material and pressure gaps between real and ideal systems in heterogeneous catalysis. Especially, ruthenium catalysts find widespread attention. Whereas they were extensively investigated for hydrogenation reactions, such as Fischer–Tropsch synthesis [1] or ammonia synthesis [2], recently the interest is focused on the application as oxidation catalysts. The oxidation of CO was chosen as a simple model reaction, which can be studied easily both on single crystal surfaces and over supported Ru catalysts.

The obtained results can be summarized as follows. Under UHV conditions Ru single crystals are not active in CO oxidation [3]. In contrast, under atmospheric pressure, supported Ru catalysts are highly active [4,5]. Furthermore, under atmospheric pressure,

---

* Corresponding author. Tel.: +49-234-32-28754;
fax: +49-234-32-14115.
E-mail address: muhler@techem.ruhr-uni-bochum.de (M. Muhler).

0920-5861/$ – see front matter © 2003 Elsevier B.V. All rights reserved.
doi:10.1016/S0920-5861(03)00391-2

Peden and Goodman [6] showed that the kinetics for Ru single crystals is comparable with the kinetics obtained for supported Ru particles on SiO_2. The observed difference in activity for single crystals is not due to a pressure gap. In fact, the high activity of Ru single crystals originates from the presence of the $RuO_2(1\,1\,0)$ surface [7,8], which is formed as a thin epitaxial overlayer on Ru(0 0 0 1) under high O_2 exposures at temperatures above 600 K [9]. An atomistic mechanism leading to $RuO_2(1\,1\,0)$ oxide patches on Ru(0 0 0 1) was proposed by Reuter et al. [10]. In a series of further studies, adsorption characteristics of CO, the properties of the various oxygen species as well as the catalytically active coordinatively unsaturated Ru sites on the $RuO_2(1\,1\,0)$ surface were investigated [11–16].

In addition, the stability of the $RuO_2(1\,1\,0)$ surface as a function of the oxygen pressure was derived using density-functional theory [17]. Recently, Reuter and Scheffler [18] constructed a phase diagram of surface structures from ultra-high vacuum to technically relevant pressures and temperatures using ab initio atomistic thermodynamics. The absence of a pressure gap was confirmed by Wang et al. [19]. The kinetic behavior of a $RuO_2(1\,1\,0)$ single crystal surface investigated at 10^{-7} mbar pressure was compared with that of small supported RuO_2 particles working at atmospheric pressure. The latter were shown to be very active in the oxidation of CO already at room temperature [20]. Virtually identical results for ideal and real Ru catalysts were also found by Madhavaram et al. [21] comparing the behavior of $RuO_2(1\,1\,0)$ single crystals with that of polycrystalline RuO_2 in the oxidation of CO and methanol. From the results summarized above, it is obvious that Ru single crystal surfaces are rather well investigated. In contrast, only little information exists concerning the behavior of real Ru catalysts in oxidation reactions under vacuum conditions as well as at high pressure [20,21].

In the present work we investigated the influence of the total pressure and of the support on the CO oxidation. Therefore, Ru nanoparticles were prepared on MgO and on SiO_2 by chemical vapor deposition. To the best of our knowledge, the adsorption of CO on Ru catalysts was only investigated so far using transmission IR spectroscopy under high-vacuum conditions. To investigate the influence of the total pressure the adsorption of CO was carried out at atmospheric pressure and monitored by in situ DRIFT (diffuse reflectance infrared Fourier transform) spectroscopy. The adsorption sites as a function of different pretreatment conditions were identified, and compared with the $RuO_2(1\,1\,0)$ single crystal surface. For the first time, continuous flow experiments were carried out in the TAP (temporal analysis of products) reactor to determine the catalytic activity at different temperatures. Due to the high-vacuum conditions these kinetic measurements were not impaired by heat and mass transfer limitations. The resulting turnover frequencies were combined with data reported for the CO oxidation at atmospheric pressure on supported Ru catalysts and on Ru single crystals in an Arrhenius plot. The good agreement suggests that the pressure and the material gaps were bridged successfully.

2. Experimental

2.1. Catalyst preparation

The catalysts Ru/MgO and Ru/SiO_2 were prepared by the MOCVD (molecular organic chemical vapor deposition) method, which was already applied successfully for the preparation of Ru/MgO [22] employed in ammonia synthesis. The $Ru_3(CO)_{12}$ (Strem) precursor was deposited on the commercially available supports MgO (ALFA, purity of 99.9955%) as well as on SiO_2 (Aerosil 200, Degussa). Details about the procedure are described in Ref. [22]. A sieve fraction of 250–355 μm was used for the chemisorption and TAP measurements.

2.2. Catalyst characterization

For elemental analysis the samples were dissolved in a sodium peroxide solution. The Ru content was measured by inductively coupled plasma optical emission spectroscopy (ICP-OES). H_2 and O_2 chemisorption measurements were carried out at 298 K in a Quantachrome Autosorb 1C instrument. Prior to these measurements the catalysts were reduced in situ in hydrogen by heating up to 773 K (heating ramp 5 K/min). This temperature was maintained for 2 h. Finally, the system was evacuated for 1 h at 773 K and cooled down to 298 K. Hydrogen (purity >99.9999%) and oxygen (purity >99.998%) were supplied by Messer Griesheim. For the characterization of the supported Ru catalysts by transmission electron microscope (TEM) a Hitachi H-8100 microscope operated at 200 kV was used. The TEM images were recorded after the chemisorption measurements. The X-ray diffraction (XRD) analysis was performed using a Siemens D500 diffractometer using Cu Kα radiation. The diffraction patterns were collected in the 2θ range from 10° to 90°.

2.3. DRIFT spectroscopy

DRIFT spectra were recorded using an Unicam RS1 spectrometer equipped with a diffuse reflectance accessory, a Spectra Tech high-temperature reaction chamber and an MCT detector. The ceramic sample cup contained about 30 mg of catalyst and was covered by a water-cooled stainless steel dome with ZnS windows. The coolant temperature was maintained at 303 K. The sample temperature was controlled by a thermocouple in direct contact with the catalyst. The flow rates (between 15 and 30 N ml/min) passing through the chamber were maintained by mass flow controllers. Two four-way valves (Valco) allowed fast switching between different gases, which were supplied by Messer Griesheim (argon: purity >99.999%, 10% H_2/Ar mixture with a hydrogen purity >99.999%, 10% CO/Ne mixture with purities >99.997 and >99.999%, respectively, and a 10% O_2/Ne mixture with an oxygen purity >99.9995%). For the DRIFTS measurements all catalysts were used as powders. Before the adsorption of CO they were pretreated as follows:

1. Heating in a 10% H_2/Ar mixture with 10 K/min up to 773 K and holding this temperature for 2 h.
2. Purging with Ar at 773 K for 15 min.
3. Cooling in Ar down to 308 K.

To investigate the adsorption of CO on oxidized Ru catalysts the reduced samples were subsequently oxidized for 2 h at 308 K in a continuous 10% O_2/Ne feed followed by purging in argon for 15 min. For the adsorption of CO a continuous flow of a 10% CO/Ne gas mixture was passed through the cell at 308 K. The adsorption process was monitored in the series mode of the spectrometer allowing a continuous collection of spectra. To determine the thermal desorption of the adsorbates the sample temperature was stepwise increased in a continuous argon flow with 10 K/min and held at certain temperatures for 15 min. After each step the samples were cooled to 308 K and a spectrum was recorded. DRIFT spectra were recorded as single-beam spectra using a resolution of 4 cm^{-1} and averaging 200 scans. To obtain the spectrum of the catalyst the single-beam spectrum of the sample was divided by the background spectrum (KBr). Spectra are presented in apparent absorption units ($-\log R$). In the case of Ru/SiO_2 and SiO_2, data are reported as difference spectra obtained by subtracting the spectrum of the sample recorded before the interaction with CO from that recorded after adsorption. This was necessary because the spectrum of silica is characterized by three broad bands within the 2000–1600 cm^{-1} region. These absorptions are due to overtones (1978 and 1625 cm^{-1}) and a combination tone at 1865 cm^{-1} of lattice vibrations [23,24].

2.4. Catalytic activity measurements

The continuous flow experiments were performed in a TAP reactor (model 1b, equipped with a high-pressure assembly). A detailed description of this reactor is found in Ref. [25]. The performance of the temperature-programmed and isothermal experiments in the vacuum-flow mode allows to measure the catalytic activity without mass transfer limitations or hot spots. It has to be pointed out that the mass transport through the fixed bed occurs via Knudsen diffusion. Thus, the mean volumetric flow rate calculated from the pressure drop in the gas container amounts to only about 1 ml min^{-1}. Thus, it is possible to detect transient adsorption/desorption phenomena by solving the mass balance as a function of time.

For the measurement, 50 mg catalyst (size fraction: 250–355 μm) were placed in the isothermal zone of a modified TAP-1 microreactor [26]. The gas flow was in the range of 0.4–0.5 N ml/min. The gas mixtures used for the DRIFT spectroscopy were also used for the kinetic measurements. In addition, neon (purity >99.999%), utilized as reference gas, and hydrogen (purity >99.9999%) were used. Both gases were supplied by Messer Griesheim. On-line analysis was performed with a calibrated quadrupole mass spectrometer. The masses were scanned in the range from 1 to 60 amu. The measured intensities were converted in relative concentrations. Prior to each experiment the samples were heated in hydrogen with 5 K/min up to 773 K. This temperature was held for 14 h. In order to reduce the samples at about 1 bar the high-pressure assembly was used. Afterwards the reactor was evacuated at 773 K and the desired start temperature was adjusted. The CO conversion was measured as a function of time as well as of temperature. CO/O_2 ratios equal to 4 and 2 were chosen.

The conversion of CO and O_2 was calculated as follows:

$$\text{conversion of CO (\%)} = \frac{C_{\mathrm{CO}}^{\mathrm{in}} - C_{\mathrm{CO}}^{\mathrm{out}}}{C_{\mathrm{CO}}^{\mathrm{in}}} \times 100 \qquad (1)$$

$$\text{conversion of } O_2 \text{ (\%)} = \frac{C_{\mathrm{O_2}}^{\mathrm{in}} - C_{\mathrm{O_2}}^{\mathrm{out}}}{C_{\mathrm{O_2}}^{\mathrm{in}}} \times 100 \qquad (2)$$

The calculation of the yield of CO_2 was based on the inlet concentration of CO ($C_{\mathrm{CO}}^{\mathrm{in}}$):

$$\text{yield of } CO_2 \text{ (\%)} = \frac{C_{\mathrm{CO_2}}^{\mathrm{out}} - C_{\mathrm{CO_2}}^{\mathrm{in}}}{C_{\mathrm{CO}}^{\mathrm{in}}} \times 100 \qquad (3)$$

Thus, at a CO/O_2 ratio equal to 4, the maximum theoretical yield of CO_2 is 50%.

3. Results and discussion

3.1. Catalyst characterization

The diffraction patterns of the Ru catalysts (Figs. 1 and 2) do not provide any evidence for the presence of Ru particles. In the case of Ru/MgO, all five sharp reflections can be assigned to crystalline MgO [27]. The diffraction pattern of Ru/SiO_2 shows only a broad reflection which originates from the amorphous support [28]. The absence of Ru reflections indicates that the size of the Ru particles is below the XRD detection limit of about 4 nm. Static H_2 chemisorption was used to determine the specific metal surface, the dispersion and the ruthenium particle size based on the extrapolation method. In addition, a surface stoichiometry of $H_{\mathrm{ads}}/Ru_{\mathrm{surf}} = 1$, a metal density of 12.3 g/cm^3 and an average area of 8.17 Å^2 per Ru atom were assumed [29,30]. The results of the chemisorption measurements are summarized in Table 1. A high Ru dispersion (63 and 69%) is found for both catalysts. The calculated average crystallite size is about 1.5 nm assuming spherical particles and is compatible with the XRD results.

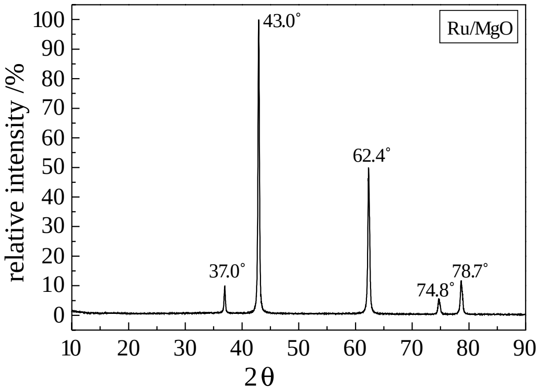

Fig. 1. XRD pattern for Ru/MgO.

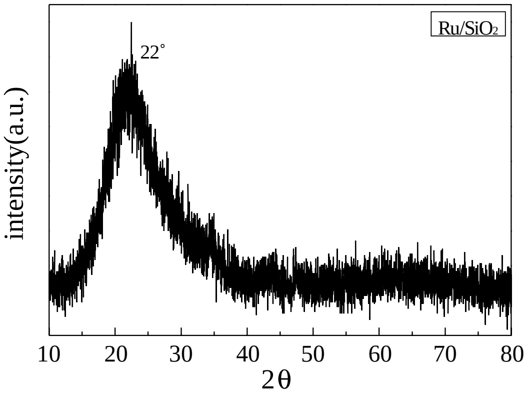

Fig. 2. XRD pattern for Ru/SiO_2.

For Ru/SiO_2 a reversible and irreversible hydrogen spillover on the support is described in the literature [31,32]. The weakly and reversibly bound hydrogen

Table 1
Results of the elemental analysis and the chemisorption measurements

Catalyst	Ru/MgO	Ru/SiO_2
Metal content (%)	3.21	3.02
H_2 adsorption (μmol g_{cat}^{-1})	101	102
Specific metal surface area (m^2 g_{cat}^{-1})	9.9	10.2
Dispersion (%)	63.4	68.5
Average crystallite size (nm)	1.6	1.5
O_2 adsorption (μmol g_{cat}^{-1})	206	197

is subtracted by the extrapolation method used in this work. However, an irreversible hydrogen spillover onto the support might lead to an overestimation of the Ru metal surface. Therefore, Uner et al. [31] suggested optimized experimental parameters to avoid this problem. With the exception of the temperature, our experimental conditions were in good agreement with these parameters. Thus, contributions from irreversible hydrogen spillover onto SiO_2 are assumed to be minimized.

The TEM micrographs of the Ru catalysts in Figs. 3 and 4 confirm the small size of the supported Ru particles. In the case of Ru/SiO_2, a mean particle size of 2.5 nm was determined from the particle size distribution in Fig. 4. For the system Ru/MgO, a Ru particle size of 1 nm or less was estimated from the particle size distribution in Fig. 3 taking into account that for a particle diameter less than 1 nm a determination of the particle diameter was not possible.

O_2 chemisorption measurements were carried out at 298 K to determine the oxygen uptake of both Ru catalysts. Based on the results (Table 1), the degree of oxidation of the O_2-treated samples used for the DRIFTS experiments was calculated. It was not the aim to determine the specific Ru metal surface which would be possible using the low-temperature oxygen chemisorption (LTOC) technique as supplement to the H_2 chemisorption measurements [33,34].

Using the extrapolation method a O/Ru_{tot} atom ratio of 1.3 was found for both catalysts, where Ru_{tot} designates the total number of ruthenium atoms in the sample. Similar results were reported for alumina-supported ruthenium catalysts with a crystallite size of 1–2 nm [34]. Including only the Ru surface atoms (Ru_{surf}) in our calculations, O/Ru_{surf} ratios of 2.0 and 1.9 are derived for Ru/MgO and Ru/SiO_2, respectively. The number of Ru surface atoms is known from the H_2 chemisorption measurements (Table 1). These results indicate the formation of a thin RuO_2 surface layer as a consequence of oxidizing the Ru catalysts at about 300 K. It was shown by a subsequent H_2 chemisorption experiment that the oxidation at room temperature did not change the Ru particle size. An oxygen to surface ruthenium stoichiometry of 2 was also found by Masthan et al. [33] using the LTOC technique for Ru/Al_2O_3 catalysts. Values of 2.14–3.5 for O/Ru_{surf} ratios were obtained by Goodwin [35] from oxygen uptake measurements at room temperature for $Ru/\gamma\text{-}Al_2O_3$. In comparison to our results, these O/Ru_{surf} ratios are somewhat higher.

3.2. DRIFT spectroscopy

In the first part of this section the adsorption of CO on the reduced Ru catalysts is compared with that on the pure supports. In the second part of the DRIFTS study adsorption of CO on oxidized Ru samples is discussed.

3.2.1. Comparison between MgO and the reduced Ru/MgO sample

After the pretreatment of MgO and Ru/MgO no bands due to adsorbates are observed. The spectra recorded before the adsorption of CO (not shown) were only characterized by one band at 3750 cm^{-1}, which is typically for O–H stretching vibrations of free OH groups of MgO [36,37]. The DRIFT spectrum of MgO between 2400 and 1100 cm^{-1} recorded during CO adsorption at 308 K is shown in Fig. 5b. In the region of carbonyl vibrations weak bands can be observed at about 2064 cm^{-1}, which disappeared after purging with Ar (not shown). These bands were assigned to an adsorbate species which contain a ketenic chromophore [38]. Between 1800 and 1200 cm^{-1} different bands indicate that carbonates are formed. This observation is in agreement with literature data [23,38–41]. Table 2 summarizes the assignment of the bands observed also after adsorption of CO_2 on MgO.

Table 2
Assignment of the bands observed after adsorption of CO on MgO

This work (cm^{-1})	Literature data (cm^{-1})	Assignment
2064	2064 [38]	Ketenic chromophore
1685	1680 [23]; 1690 [40]	Bidentate carbonate
1660	1666–1655 [60–62]	Bidentate carbonate
1628	1630 [61]	Bidentate carbonate
1307	1310 [23,40]	Bidentate carbonate
1275	1275 [40,61]	Bidentate carbonate
1518	1520 [40]; 1517 [60,61]	Unidentate carbonate
1398	1398 [60,61]	Unidentate carbonate
1370	1370 [40]	Unidentate carbonate
1215	1210 [23]; 1220 [60]	Bicarbonate

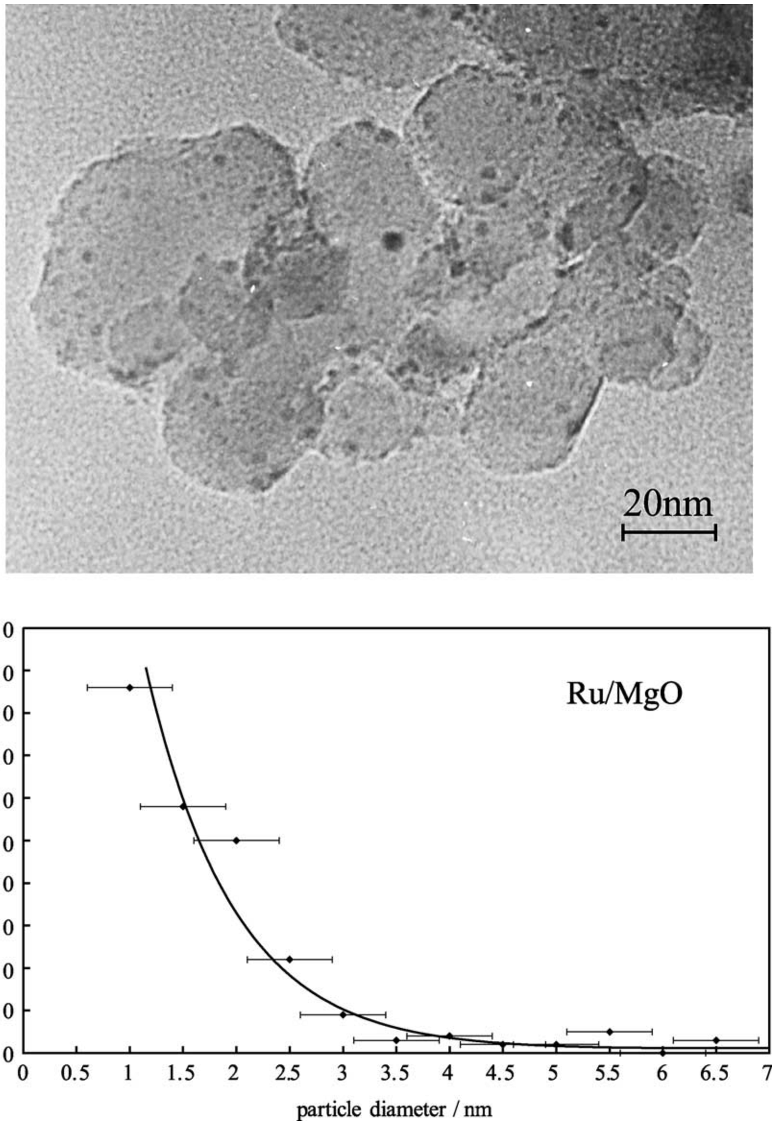

Fig. 3. TEM image and particle size distribution of Ru/MgO.

The spectrum of CO adsorbed on Ru/MgO is shown in Fig. 5a. In the region of carbonyl vibrations the spectrum is characterized by two sharp bands (2134 and 2052 cm^{-1}) and a broad shoulder at about 1950 cm^{-1}. The band at 2052 cm^{-1} is due to C–O vibrations of linearly adsorbed CO on reduced Ru sites. This assignment is confirmed by an FT-IRAS study of CO adsorption on Ru(0 0 0 1) single crystals [42]. In this study, Peden et al. [42] observed a band at 2060 cm^{-1} and assigned it to linearly bound CO. The broad shoulder at 1950 cm^{-1} was assigned to bridged CO. The sharp band at 2134 cm^{-1} with lower intensity points to CO adsorbed on oxidized Ru sites (Ru^{n+}) as shown later in this study.

In addition to the discussed bands in the carbonyl region, different bands between 1200 and 1800 cm^{-1} indicate the formation of carbonates, which was already observed after CO adsorption on MgO. In comparison to MgO, the positions and intensities of the carbonate bands are very similar. Obviously, the

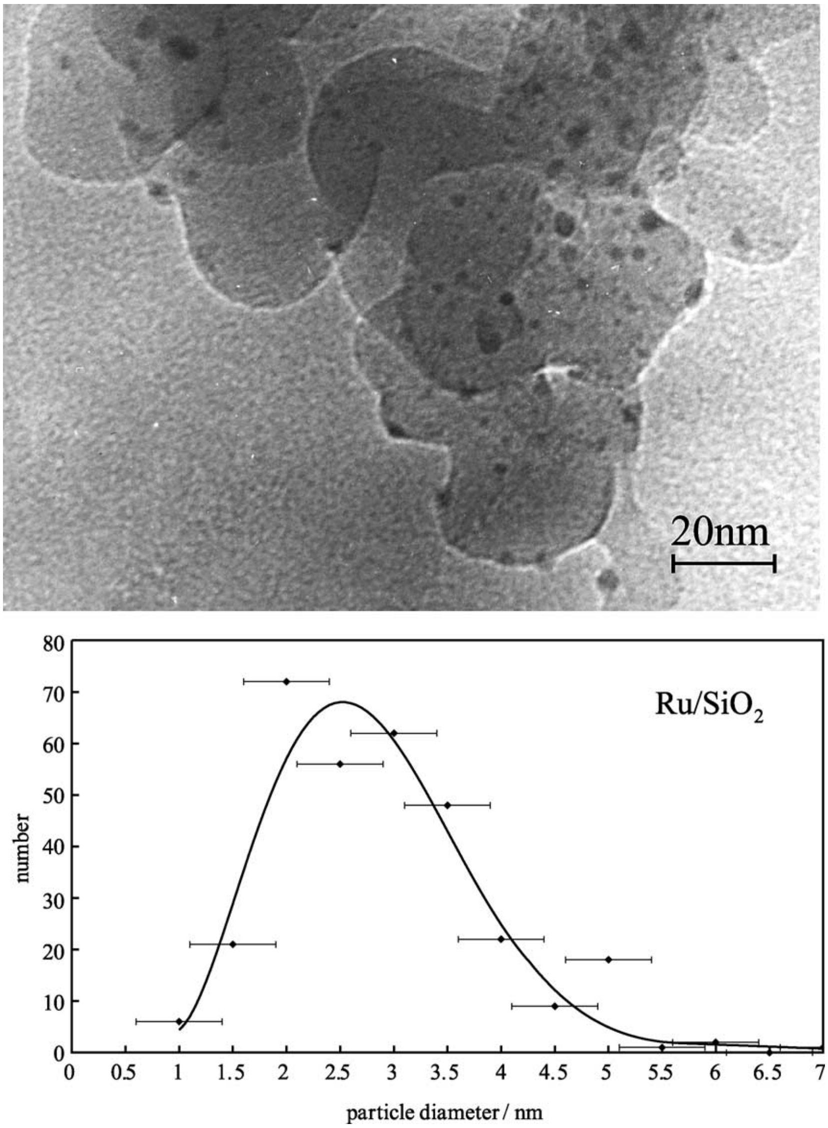

Fig. 4. TEM image and particle size distribution of Ru/SiO$_2$.

presence of Ru particles has no important influence on the formation of carbonates on the support.

To study the thermal desorption of the different adsorbates the CO-covered Ru/MgO catalyst was heated in a continuous Ar flow up to elevated temperatures. The corresponding DRIFT spectra are shown in Fig. 6. At 373 K (Fig. 6b) the band at 2134 cm^{-1} is no longer present. This implies that CO adsorbed on Ru^{n+} sites is very weakly bound, which confirms the explanation given above. The band at 2048 cm^{-1} (linearly adsorbed CO on Ru^0 sites) is shifted to lower wavenumbers with increasing desorption temperature and disappeared nearly completely at 673 K (Fig. 6e). This red-shift may be explained by a decrease of the CO coverage or can be attributed to the transformation of the linearly bound CO to the bridged bound CO. The small change in intensity of the corresponding IR band observed at lower temperatures (Fig. 6a–c)

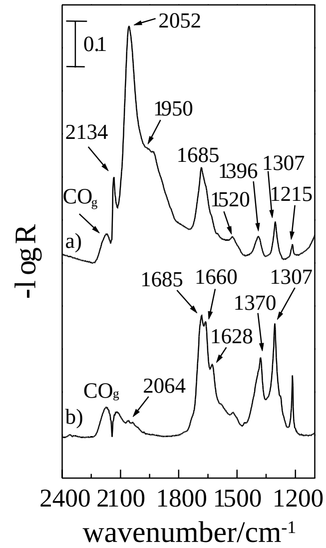

Fig. 5. DRIFT spectra after 15 min adsorption of CO at 308 K: (a) Ru/MgO and (b) MgO.

suggests that below 473 K transformation rather than desorption is dominant. The broad shoulder at 1950 cm^{-1} reveals a composite nature and splits into several components at 1919 and 1883 cm^{-1} at 773 K (Fig. 6f).

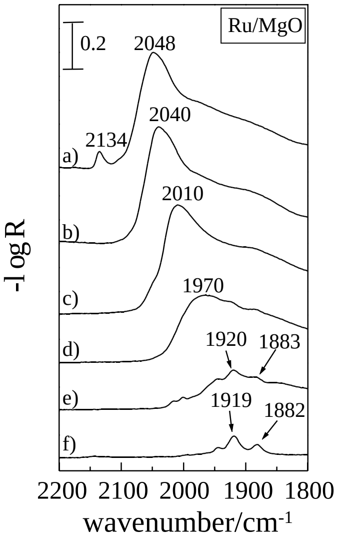

Fig. 6. DRIFT spectra of Ru/MgO after adsorption of CO followed by desorption in Ar at: (a) 308 K, (b) 373 K, (c) 473 K, (d) 573 K, (e) 673 K and (f) 773 K.

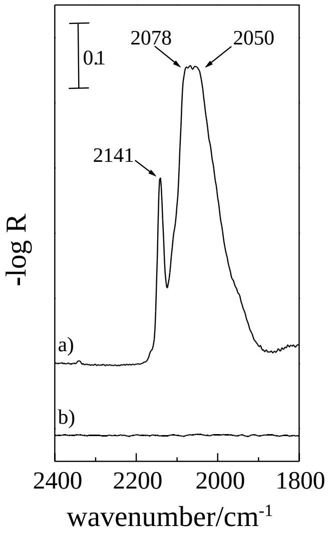

Fig. 7. DRIFT difference spectra after 15 min adsorption of CO at 308 K and purging with Ar: (a) Ru/SiO$_2$ and (b) SiO$_2$.

3.2.2. Comparison between SiO$_2$ and the reduced Ru/SiO$_2$ sample

After the pretreatment, the spectra of SiO$_2$ and Ru/SiO$_2$ (not shown) were characterized by the typical sharp band at 3745 cm^{-1} assigned to O–H stretching vibrations [43]. Broad bands below 2200 cm^{-1} were due to lattice vibrations. The difference spectra of the SiO$_2$ and Ru/SiO$_2$ samples after the adsorption of CO at 308 K and purging with Ar are shown in Fig. 7b and a, respectively. Only the region of carbonyl vibrations is presented because in the carbonate region no bands were observed. Thus, in contrast to the basic MgO, the more acidic SiO$_2$ is inert for the adsorption of CO due to the stronger Si–O bond.

The spectrum of Ru/SiO$_2$ (Fig. 7a) shows three bands (2141, 2078 and 2050 cm^{-1}) with overlapping bands at 2078 and 2050 cm^{-1}. In addition, a small shoulder at 1950 cm^{-1} can be observed. These bands are due to C–O vibrations of adsorbed CO on different Ru sites. The assignment of the observed bands is summarized in Table 3. The stability of the adsorbed CO species on Ru/SiO$_2$ was ascertained by heating the sample in Ar to higher temperatures. The results (not shown) are in good agreement with TPD and IR data obtained by Yokomizo et al. [44]: CO adsorbed on oxidized Ru^{n+} sites desorbs between 300 and 475 K,

Table 3
Assignment of the bands observed after adsorption of CO on reduced Ru/SiO_2

This work (cm^{-1})	Literature data (cm^{-1})	References	Assignment
2141/2078	2132, 2070	[5]	$Ru^{n+}(CO)_2$
	2140–2130, 2080–2070	[47]	$Ru^{1+}(CO)_2$
	2146, 2085	[63]	$Ru^{n+}(CO)_2$
	2130, 2064	[24]	$Ru^{n+}(CO)_3$
	2144, 2082	[45,46]	$Ru^{2+}(CO)_3$
2050	2040 ± 10	[24,46–49]	Ru^0–CO
1950 (shoulder)	1900–1700	[63]	Bridged CO

whereas linearly adsorbed CO on Ru^0 sites desorbs at higher temperatures with the maximum desorption rate at about 520 K.

3.2.3. *Adsorption of CO on the oxidized Ru catalysts*

To study the adsorption of CO under conditions relevant for the catalytic oxidation, CO was passed through the IR cell filled with the in situ oxidized Ru catalysts. As determined by O_2 chemisorption (Table 1) the oxidized catalysts are characterized by a thin RuO_2 surface layer. In Fig. 8 the spectra of oxidized Ru/MgO during adsorption of CO are presented as a function of time. At the beginning of the adsorption process, two bands in the carbonyl region can be observed at 2125 and 2072 cm^{-1}. At lower wavenumbers a weak shoulder is noticeable. In addition, gaseous CO_2 and gaseous CO were detected. Particularly during the first three minutes, CO was converted to CO_2. Even after 30 min minor amounts of CO_2 were detected which is in agreement with the change of the bands between 2200 and 1800 cm^{-1}. A new band arose at about 1995 cm^{-1} and its intensity increased during adsorption. Obviously, the bands at 2125 and 2072 cm^{-1} can be assigned to CO adsorbed on Ru^{n+} sites, whereas the new band at ca. 1995 cm^{-1} is due to CO adsorbed on oxygen vacancies formed by the oxidation of CO to CO_2. Hence, we can conclude that the adsorption of CO on oxidized Ru/MgO at 308 K leads to a partial reduction of the RuO_2 surface layer.

For Ru/SiO_2 we observed a similar behavior. The difference spectra as a function of time are shown in Fig. 9. They are characterized by sharp bands with high intensity at 2130 and 2074 cm^{-1}. In agreement with the literature these bands can be assigned to adsorbed CO on Ru^{n+} sites [45–50]. At 2016 cm^{-1}, another band can be observed which increases with time. This band is due to C–O vibrations of CO adsorbed on oxygen vacancies created by the reaction of oxygen with CO. Both the appearance of this new band and the formation of gaseous CO_2 during the CO treatment indicate that CO was oxidized associated with a reduction of the RuO_2 surface.

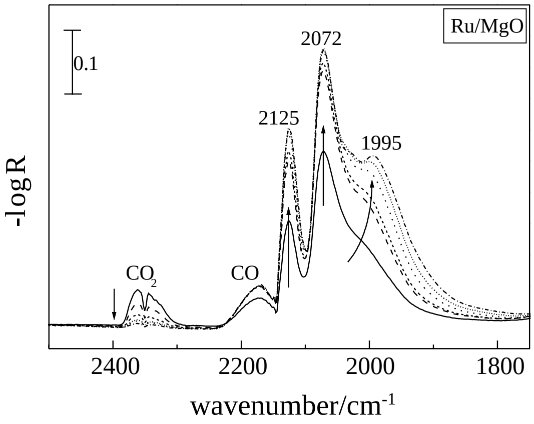

Fig. 8. DRIFT spectra of oxidized Ru/MgO in dependence on the CO adsorption time. Spectra were recorded after 1 min (solid line), 2 min (long dashes), 3 min (short dashes), 10 min (dotted), 20 min (short dotted) and 30 min (dash-dotted) adsorption of CO.

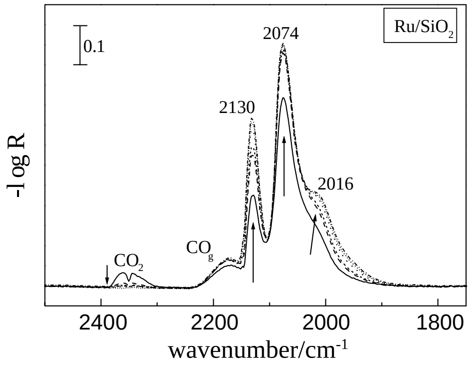

Fig. 9. DRIFT difference spectra of oxidized Ru/SiO_2 in dependence on the CO adsorption time. Spectra were recorded after 1 min (solid line), 2 min (long dashes), 3 min (short dashes), 10 min (dotted), 20 min (short-dotted) and 30 min (dash-dotted) adsorption of CO.

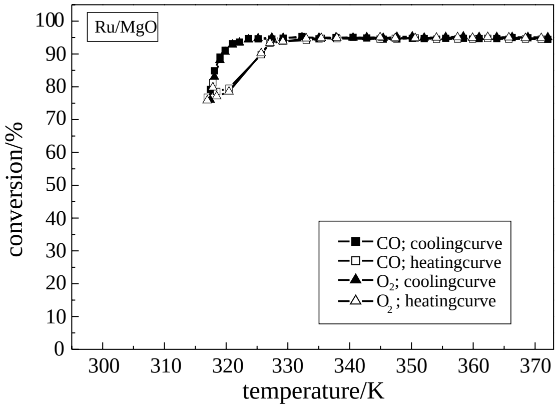

Fig. 10. CO and O_2 conversion for the oxidation of CO over 50 mg Ru/MgO as a function of temperature. The CO/O_2 reactant feed ratio was 2.

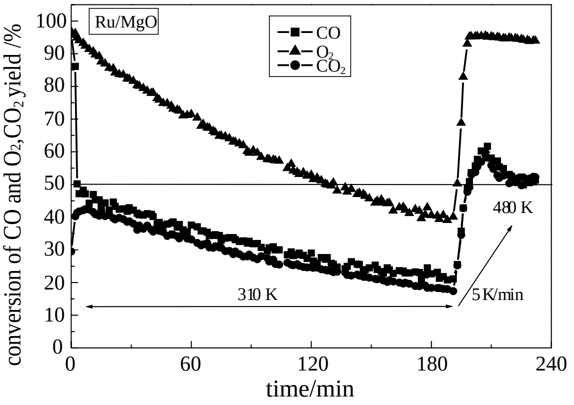

Fig. 12. CO and O_2 conversion and CO_2 yield for the oxidation of CO as a function of time and temperature over Ru/MgO. The CO/O_2 reactant feed ratio was 4.

3.3. Catalytic activity measurements

The temperature-programmed flow experiments were carried out to determine the kinetically controlled region under the specific experimental conditions used in this study. The experiments were started at higher temperatures (>625 K) cooling at a rate of 2 K/min to 310 K followed by a heating at 2 K/min to 625 K. In Figs. 10 and 11, CO and O_2 conversions in an experiment with a CO/O_2 ratio of 2 are shown for Ru/MgO and Ru/SiO_2, respectively. The figures are restricted to temperatures between 273 and 373 K because above these temperatures full conversion was reached with both supported Ru catalysts. A decrease of the degree of conversion was only observed for temperatures below 350 K. A closer inspection of the kinetic data below 350 K reveals that the catalytic activity of both samples is almost the same. The hysteresis between the cooling and the heating branch indicates that both catalysts deactivate at low temperatures. However, the increase to essentially 100% conversion of CO and O_2 when heating up again proves that the deactivation at room temperature is reversible for both catalysts.

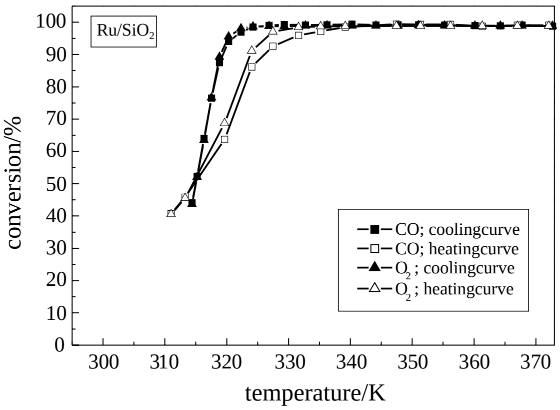

Fig. 11. CO and O_2 conversion for the oxidation of CO over 50 mg Ru/SiO_2 as a function of temperature. The CO/O_2 reactant feed ratio was 2.

Furthermore, the time dependence of the oxidation of CO was investigated at different temperatures. In this case, a CO/O_2 ratio of 4 was used. In Fig. 12 the results obtained with Ru/MgO are presented. At the beginning of the experiment a degree of CO conversion of more than 80% was observed at 310 K. Simultaneously, only a small amount of CO_2 was formed indicating that CO was mainly adsorbed on the catalyst, but not oxidized to CO_2. The deficit in the CO_2 yield at the beginning of the experiment can be explained by the formation of carbonates on MgO. The observed discrepancies in the carbon and oxygen mass balance are in agreement with these explanations. In addition, it can be concluded that also adsorbed oxygen has not completely reacted to CO_2. Coke formation at temperatures lower than 423 K can be excluded [51,52].

For both catalysts a deactivation with time on stream at room temperature was observed. In the case of Ru/SiO_2, steady state was reached after 3 h

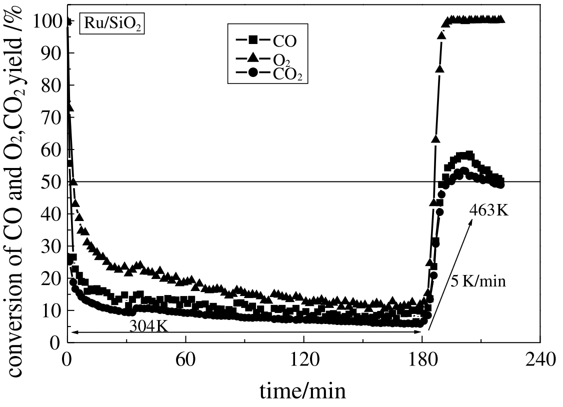

Fig. 13. CO and O_2 conversion and CO_2 yield for the oxidation of CO as a function of time and temperature over Ru/SiO_2. The CO/O_2 reactant feed ratio was 4.

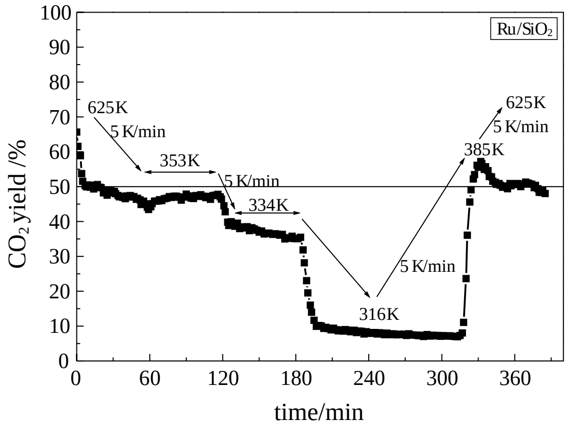

Fig. 14. CO_2 yield for the oxidation of CO as a function of time and temperature over Ru/SiO_2. The CO/O_2 reactant feed ratio was 4.

yielding 7% CO (Fig. 13). The deactivation process was slower for Ru/MgO (Fig. 12). After 3 h steady state was not yet reached. This observation and the temperature difference (310 K instead of 304 K) can explain the slightly higher CO_2 yield (18% after 3 h) compared to the results obtained with Ru/SiO_2.

During the subsequent heating ramp (5 K/min to ca. 473 K), an increase of the CO and O_2 conversion and also of the CO_2 yield was observed for both catalysts. At about 350 K the CO_2 yield reached values above 50% for a short period of time. Concomitantly, the CO conversion exceeded the maximum theoretical value of 50% and a discrepancy in the oxygen mass balance was observed. These observations suggest that oxygen which was adsorbed initially reacted at higher temperatures. After the consumption of excess oxygen, the CO_2 yield decreased to the maximum theoretical yield of 50%. It has to be mentioned that Kiss and Gonzalez [5] reported an irreversible deactivation of a Ru/SiO_2 catalyst for the oxidation of CO at atmospheric pressure. This observation is in contrast to our results observed under high vacuum.

In the kinetically controlled region, steady-state degrees of conversion were determined with both catalysts and at different CO/O_2 reactant feed ratios (CO/O_2 = 2 and 4). For example, the CO_2 yield is shown in Fig. 14 obtained with Ru/SiO_2. As expected at higher temperatures, the CO_2 yield is close to the maximum theoretical value. Even at 353 K, a CO_2 yield of almost 50% was observed. Therefore, only the steady-state values obtained at 334 and 316 K (Fig. 14) were converted into turnover frequencies (TOF = number of CO_2 molecules per metal surface site per second). These values are shown in the Arrhenius plot (Fig. 15) together with other turnover frequencies derived in this study. In addition, reported data obtained in high pressure studies on a Ru(0 0 0 1) single crystal surface [6] and on silica-supported ruthenium catalysts prepared by impregnation [4,5] are presented. The turnover frequencies for Ru/SiO_2

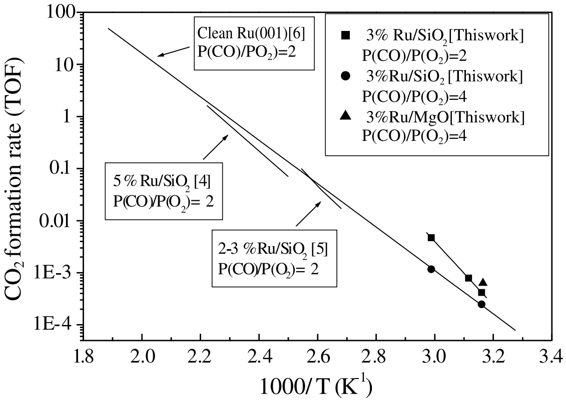

Fig. 15. Arrhenius plot of the rates of CO_2 formation (TOF = turnover frequency, number of CO_2 molecules formed per metal surface site per second) over the Ru/SiO_2 catalyst for different CO/O_2 reactant feed ratios. Also included: data obtained on a Ru(0 0 0 1) catalyst [6] and two silica-supported ruthenium catalysts prepared by impregnation [4,5].

and Ru/MgO are rather similar and there is a very good agreement regarding the slope (activation energy of 81.6 kJ/mol [6]) as well as the absolute scale comparing our results with the literature data. This clearly proves the absence of a pressure gap. Furthermore, the activation energy depends on the CO/O_2 reactant feed ratio which was also reported for the Ru single crystals [6].

4. Discussion

In the first part of Section 3.2 we compared the adsorption of CO on the reduced Ru catalysts with that on the pure supports. For both reduced Ru catalysts, the adsorption of CO on Ru^{n+} sites was observed. However, the number of these sites was dependent on the support. The existence of Ru^{n+} sites after complete reduction of the sample is not fully understood, but was also observed by Schwank et al. [53] for Ru/MgO as well as for Ru/SiO_2 by Yokomizo et al. [46] in the presence of CO.

For Ru/SiO_2, the formation of oxidized Ru^{n+} sites was explained by corrosive chemisorption [46]:

$$\mathrm{Ru} + 2\mathrm{Si{-}OH} + 3\mathrm{CO} \rightleftharpoons (\mathrm{SiO})_2\mathrm{Ru}(\mathrm{CO})_3 + \mathrm{H}_2 \qquad (4)$$

However, this mechanism was critically discussed and modified by Kantcheva and Sayan [24] who assume that the influence of SiO_2 (particularly the influence of the silanol groups) on the adsorption of CO on Ru/SiO_2 cannot be neglected. Taking into account that the existence of Ru^{n+} sites in spite of a reductive pretreatment was also reported for titania-supported Ru [54] and for Ru supported on dealuminated Y zeolite [45], the formation of these sites is not restricted to a special support. However, the type of the support determines the number of Ru^{n+} sites which are formed during adsorption of CO. The existence of Ru^{n+} sites after reduction in the absence of CO is rather unlikely, because the same Ru/MgO sample was successfully applied in ammonia synthesis after reduction in hydrogen at 773 K [22]. Taking into consideration that a partially oxidized Ru catalyst would be hardly active in ammonia synthesis, it can be safely assumed that the reduction of the Ru catalysts was complete. Thus, the formation of Ru^{n+} sites is presumably induced by the adsorption of CO according to the corrosive chemisorption mechanism.

To reveal the influence of the total pressure on the adsorption of CO our results are compared with reported data obtained under high-vacuum conditions using transmission IR spectroscopy. In addition to the difference in pressure, in transmission IR studies the samples were pressed into self-supporting wafers whereas it is possible to use untreated powders in DRIFTS studies. Despite all differences between both IR methods, the observed band positions as well as the assignment to differently CO species adsorbed on various Ru sites are in a very good agreement. Particularly, the transmission IR study described by Guglielminotti [55] for Ru/MgO corresponds well with our assignment. In addition, the adsorption of bridged CO on Ru/MgO was also observed by Mizushima et al. [56] who determined an exact geometry for this species by EXAFS.

The comparison between our assignment of the vibration frequencies of adsorbed CO on Ru/SiO_2 and data reported for IR experiments carried out under high vacuum is presented in Table 2. Concerning the position of the bands there is again good agreement, indicating the absence of a pressure gap. It has to be mentioned that the assignment of the two high-frequency (HF) bands at ca. 2140 and 2080 cm^{-1} reported in several studies is contradictory. Because of the overlapping bands observed in the DRIFT spectra we were not able to distinguish between the different assignments. However, we favor the assignment to a Ru tricarbonyl $Ru^{2+}(CO)_3$ as suggested by Landmesser and Miessner [45] who studied the interaction of CO with ruthenium supported on dealuminated Y zeolite. Using this zeolite unusual sharp CO stretching bands were obtained.

Summarizing the results given above, the DRIFT spectra show that the adsorption of CO on reduced Ru supported catalysts is clearly influenced by the nature of the support. Carbonates were only formed on Ru/MgO due to the basic properties of the support. Oxidized Ru sites were found to a greater extent on Ru/SiO_2. In addition, bridged CO was mainly observed on Ru/MgO which may be related to the different shape of the particle size distribution or to electronic reasons. It is known that the bridge-bound CO is favored in the case of increasing particle size [57]. This interpretation does not seem to hold for Ru/MgO because the Ru particle size is smaller compared to Ru/SiO_2. Thus, electronic reasons are presumably decisive for the different adsorption geometry of CO. The influence of different promoters and supports was already demonstrated for Ru catalysts in ammonia synthesis [22]. Independent of the support, we found a good agreement with data reported for transmission IR experiments carried out under high vacuum. This result points to the absence of a pressure gap.

Regarding the results of the adsorption of CO on the oxidized Ru catalysts (Figs. 8 and 9) not only a significantly weaker influence of the support can be observed in contrast to the adsorption on the reduced catalysts. In addition, the bands of CO molecules adsorbed on oxidized samples appear at lower wavenumbers compared with those of the CO–Ru^{n+} species formed on the reduced samples. This shift might be explained by a lower CO coverage on the oxidized samples. However, literature data show that the high frequency bands (2130 and 2080 cm^{-1}) are not dependent on CO coverage [46]. Yokomizo et al. [46] propose that the oxidized Ru sites on reduced Ru/SiO_2 which were the consequence of a corrosive chemisorption process should be more highly oxidized than the Ru^{n+} atoms on the oxidized surface of the Ru particles. The latter might be present as $(RuO)_2Ru(CO)_3$ species as suggested by Yokomizo et al. [46] or as a RuO_x surface similar to the well investigated $RuO_2(1\,1\,0)$ single crystal surface [7]. Thus, the observed red-shift of the carbonyl bands on the oxidized Ru samples may be explained by the decrease of the oxidation state of the Ru^{n+} sites [58].

The formation of the thin RuO_2 surface layer on the Ru catalysts as determined by O_2 chemisorption (Table 1) and its supposed similarity with the $RuO_2(1\,1\,0)$ single crystal surface requires a more detailed comparison: the CO vibration frequencies of CO adsorbed on the supported catalysts and the $RuO_2(1\,1\,0)$ single crystal surface are summarized in Table 4. For the ideal single crystal surface it was possible to identify exactly the adsorption sites and the adsorption geometry of CO [59]. At higher CO coverages, only the adsorption of CO in the asymmetric bridge position was observed. This explains the absence of a band at about 1900 cm^{-1} in the DRIFT spectra. The fact that we observed two HF bands instead of only one band found in the single crystal studies can be explained by the formation of a multicarbonyl, most likely a tricarbonyl [45], on the supported Ru catalysts. Our conclusion that the RuO_2 surface layer is partially reduced by the exposure to CO, as indicated by the increase of a new band at about 1995 cm^{-1}, is also confirmed by the single crystal data. Seitsonen et al. [59] report that the adsorption of CO in symmetric bridge and asymmetric bridge positions is only possible on the reduced $RuO_2(1\,1\,0)$ surface. Thus, the ideal $RuO_2(1\,1\,0)$ single crystal surface and the RuO_2 surface layer formed on Ru/MgO and Ru/SiO_2 at room temperature in flowing O_2 seem to be rather similar.

This similarity is further supported by the catalytic measurements. Related to the Ru metal surface ($Ru/SiO_2 = 10.2\,m^2/g$), the reaction rate for the oxidation of CO with a CO/O_2 reactant feed ratio of 2 at 321 K is of the order of $\approx 10^{12}$ molecules $cm^{-2}\,s^{-1}$ which is in agreement with reaction rates published recently by Wang et al. [19] for the oxidation of CO on a $RuO_2(1\,1\,0)$ single crystal surface under UHV conditions. Thus, in addition to the similar activation energy for Ru single crystals and supported Ru catalysts presented in the Arrhenius plot (Fig. 15), the absolute reaction rate is in good agreement. Therefore, we can assume that the active phase for the oxidation of CO is supported RuO_2. Further studies are in progress to derive the precise degree of oxidation of the supported Ru particles under steady-state reaction conditions as a function of the total pressure, and to elucidate the deactivation phenomena observed by Kiss and Gonzalez [5] at atmospheric pressure.

Table 4
Bridging the material gap: comparison of CO vibration frequencies (cm^{-1}) of adsorbed CO on the oxidized Ru catalysts and on the $RuO_2(1\,1\,0)$ single crystal surface

Ru/MgO (DRIFTS)	Ru/SiO_2 (DRIFTS)	$RuO_2(1\,1\,0)$ (HREELS) [14]	$RuO_2(1\,1\,0)$ (DFT) [59]	$RuO_2(1\,1\,0)$ (LEED) [59]
2125/2072	2130/2074	2115	2085	On-top
1995	2016	1975/1895	1994/1897	Asymmetric/symmetric bridge

5. Conclusions

The chemical vapor deposition of $Ru_3(CO)_{12}$ was found to be a suitable synthesis method to achieve a high Ru metal dispersion on both MgO and SiO_2. In situ DRIFTS measurements carried out at room temperature showed that the adsorption of CO on the reduced Ru catalysts is clearly influenced by the support. Carbonate formation only takes place on the more basic MgO. In addition, bridged bound CO was mainly found on Ru/MgO, whereas the silanol groups of Ru/SiO_2 are probably responsible for the formation of a greater amount of oxidized Ru sites. The agreement between our results obtained at atmospheric pressure with results from transmission IR spectroscopy measurements under high vacuum proves that the total pressure has no influence on the adsorption behavior of CO.

In contrast to the reduced catalysts, only few differences were observed in the DRIFT spectra of CO adsorbed on the oxidized Ru samples. This observation is explained by the formation of a thin RuO_2 surface layer obtained by oxidizing the samples at 300 K. CO exposure leads to a partial reduction of this RuO_2 surface layer. Furthermore, a comparison with results obtained with the $RuO_2(1\,1\,0)$ single crystal surface under ultra-high vacuum indicates that the surface science approach is applicable to supported Ru catalysts.

The catalytic measurements under high-vacuum conditions displayed a high activity in the oxidation of CO even down to room temperature for both supported Ru catalysts. This is in agreement with the DRIFTS experiments, where the oxidation of CO was also observed at room temperature independent of the support. The derived turnover frequencies are in good agreement with reported data obtained on the $RuO_2(1\,1\,0)$ single crystal surface. Thus, supported RuO_2 is identified as the catalytically active phase. The absence of a pressure gap was clearly demonstrated by the Arrhenius diagram combining our turnover frequencies obtained under high-vacuum conditions with reported data obtained in high pressure studies.

Acknowledgements

The authors gratefully acknowledge fruitful discussions with Herbert Over and the financial support by the Deutsche Forschungsgemeinschaft (DFG, SPP 1091).

References

[1] H. Schulz, Appl. Catal. A 186 (1999) 3.
[2] O. Hinrichsen, F. Rosowski, M. Muhler, G. Ertl, Chem. Eng. Sci. 51 (1996) 1683.
[3] H.I. Lee, J.M. White, J. Catal. 63 (1980) 261.
[4] N.W. Cant, P.C. Hicks, B.S. Lennon, J. Catal. 54 (1978) 372.
[5] J.T. Kiss, R.D. Gonzalez, J. Phys. Chem. 88 (1984) 892.
[6] C.H.F. Peden, D.W. Goodman, J. Phys. Chem. 90 (1986) 1360.
[7] H. Over, Y.D. Kim, A.P. Seitsonen, S. Wendt, E. Lundgren, M. Schmid, P. Varga, A. Morgante, G. Ertl, Science 287 (2000) 1474.
[8] Y.D. Kim, H. Over, G. Krabbes, G. Ertl, Top. Catal. 14 (2001) 95.
[9] A. Böttcher, H. Niehus, Phys. Rev. B 60 (1999) 14396.
[10] K. Reuter, C. Stampfl, M.V. Ganduglia-Pirovano, M. Scheffler, Chem. Phys. Lett. 352 (2002) 311.
[11] Y.D. Kim, A.P. Seitsonen, H. Over, Phys. Rev. B 63 (2001) 115419.
[12] Y.D. Kim, A.P. Seitsonen, S. Wendt, J. Wang, C. Fan, K. Jacobi, H. Over, G. Ertl, J. Phys. Chem. B 105 (2001) 3752.
[13] C.Y. Fan, J. Wang, K. Jacobi, G. Ertl, J. Chem. Phys. 114 (2001) 10058.
[14] J. Wang, C.Y. Fan, K. Jacobi, G. Ertl, Surf. Sci. 481 (2001) 113.
[15] H. Over, A.P. Seitsonen, E. Lundgren, M. Wiklund, J.N. Andersen, Chem. Phys. Lett. 342 (2001) 467.
[16] H. Over, A.P. Seitsonen, E. Lundgren, M. Schmid, P. Varga, J. Am. Chem. Soc. 123 (2001) 11807.
[17] K. Reuter, M. Scheffler, Phys. Rev. B 65 (2002) 035406.
[18] K. Reuter, M. Scheffler, Phys. Rev. Lett. 90 (2003) 046103.
[19] J. Wang, C.Y. Fan, K. Jacobi, G. Ertl, J. Phys. Chem. B 106 (2002) 3422.
[20] L. Zang, H. Kisch, Angew. Chem. 112 (2000) 4075.
[21] H. Madhavaram, H. Idriss, S. Wendt, Y.D. Kim, M. Knapp, H. Over, J. Aßmann, E. Löffler, M. Muhler, J. Catal. 202 (2001) 296.
[22] H. Bielawa, O. Hinrichsen, A. Birkner, M. Muhler, Angew. Chem. Int. Ed. 40 (2001) 1061.
[23] D.G. Rethwisch, J.A. Dumesic, Langmuir 2 (1986) 73.
[24] M. Kantcheva, S. Sayan, Catal. Lett. 60 (1999) 27.
[25] O. Hinrichsen, A.C. van Veen, H.W. Zanthoff, M. Muhler, in: J.F. Haw (Ed.), In Situ Spectroscopy in Heterogeneous Catalysis, Wiley/VCH, Weinheim, 2002, p. 237.
[26] A.C. van Veen, H.W. Zanthoff, O. Hinrichsen, M. Muhler, J. Vac. Sci. Technol. A 19 (2) (2001) 651.
[27] M.A. Aramendia, J.A. Benitez, V. Borau, C. Jiménez, J.M. Marinas, J.R. Ruiz, F. Urbano, Langmuir 15 (1999) 1192.
[28] B.M. Reddy, K.S.P. Rao, V.M. Mastikhin, J. Catal. 113 (1988) 556.
[29] R.A. Dalla Betta, J. Catal. 34 (1974) 57.
[30] R.A. Dalla Betta, J. Phys. Chem. 79 (1975) 2519.

[31] D.O. Uner, M. Pruski, T.S. King, J. Catal. 156 (1995) 60.

[32] F. Engelke, R. Vincent, T.S. King, M. Pruski, J. Chem. Phys. 101 (1994) 7262.

[33] S.K. Masthan, K.V.R. Chary, P.K. Rao, J. Catal. 124 (1990) 289.

[34] K. Taylor, J. Catal. 38 (1975) 299.

[35] J.G. Goodwin Jr., J. Catal. 68 (1981) 227.

[36] P.J. Anderson, R.F. Horlock, J.F. Oliver, Trans. Faraday Soc. 61 (1965) 2754.

[37] Y. Kuroda, E. Yasugi, H. Aoi, K. Miura, T. Morimoto, J. Chem. Soc., Faraday Trans. I 84 (1988) 2421.

[38] E. Guglielminotti, S. Coluccia, E. Garrone, L. Cerruti, A. Zecchina, J. Chem. Soc., Faraday Trans. I 75 (1979) 96.

[39] H. Kölbel, M. Ralek, P. Jiru, Z. Naturforsch. 25a (1970) 670.

[40] R.S.C. Smart, T.L. Slager, L.H. Little, R.G. Greenler, J. Phys. Chem. 77 (1973) 1019.

[41] G.-W. Wang, H. Hattori, J. Chem. Soc., Faraday Trans. I 80 (1984) 1039.

[42] C.H.F. Peden, D.W. Goodman, M.D. Weisel, F.M. Hoffmann, Surf. Sci. 253 (1991) 44.

[43] A.J. McFarlan, B.A. Morrow, J. Phys. Chem. 95 (1991) 5388.

[44] G.H. Yokomizo, C. Louis, A.T. Bell, J. Catal. 120 (1989) 15.

[45] H. Landmesser, H. Miessner, J. Phys. Chem. 95 (1991) 10544.

[46] G.H. Yokomizo, C. Louis, A.T. Bell, J. Catal. 120 (1989) 1.

[47] A.A. Davydov, A.T. Bell, J. Catal. 49 (3) (1977) 345.

[48] M.F. Brown, R.D. Gonzalez, J. Phys. Chem. 80 (1976) 1731.

[49] H.-W. Chen, Z. Zhong, J.M. White, J. Catal. 90 (1984) 119.

[50] C. Crisafulli, R. Maggiore, S. Scire, S. Galvagno, J. Chem. Soc., Faraday Trans. 90 (1994) 2809.

[51] J.A. Rabo, A.P. Risch, M.L. Poutsma, J. Catal. 53 (1978) 295.

[52] G.G. Low, A.T. Bell, J. Catal. 57 (1979) 397.

[53] J. Schwank, G. Parravano, H.L. Gruber, J. Catal. 61 (1980) 19.

[54] J.L. Robbins, J. Catal. 115 (1989) 120.

[55] E. Guglielminotti, Langmuir 2 (1986) 812.

[56] T. Mizushima, K. Tohji, Y. Udagawa, A. Ueno, J. Am. Chem. Soc. 112 (1990) 7887.

[57] M. Bäumer, H.-J. Freund, Prog. Surf. Sci. 61 (1999) 127.

[58] G. Blyholder, J. Phys. Chem. 68 (1964) 2772.

[59] A.P. Seitsonen, Y.D. Kim, M. Knapp, S. Wendt, H. Over, Phys. Rev. B 65 (2002) 035413.

[60] J.V. Evans, T.L. Whateley, Trans. Faraday Soc. 63 (1967) 2769.

[61] H. Tsuji, T. Shishido, A. Okamura, Y. Gao, H. Hattori, H. Kita, J. Chem. Soc., Faraday Trans. 90 (1994) 803.

[62] S.J. Gregg, J.D. Ramsay, J. Chem. Soc. A (1970) 2784.

[63] H. Yamasaki, Y. Kobori, S. Naito, T. Onishi, K. Tamaru, J. Chem. Soc., Faraday Trans. I 77 (1981) 2913.